

Nondecaying linear and nonlinear modes in a periodic array of spatially localized dissipations

S. C. Fernández and V. S. Shchesnovich

Centro de Ciências Naturais e Humanas, Universidade Federal do ABC, Santo André, SP, 09210-170 Brazil

Abstract. We demonstrate the existence of extremely weakly decaying linear and nonlinear modes (i.e. modes immune to dissipation) in the one-dimensional periodic array of identical spatially localized dissipations, where the dissipation width is much smaller than the period of the array. We consider wave propagation governed by the one-dimensional Schrödinger equation in the array of identical Gaussian-shaped dissipations with three parameters, the integral dissipation strength Γ_0 , the width σ and the array period d . In the linear case, setting $\sigma \rightarrow 0$, while keeping Γ_0 fixed, we get an array of zero-width dissipations given by the Dirac delta-functions, i.e. the complex Kroning-Penney model, where an infinite number of nondecaying modes appear with the Bloch index being either at the center, $k = 0$, or at the boundary, $k = \pi/d$, of an analog of the Brillouin zone. By using numerical simulations we confirm that the weakly decaying modes persist for σ such that $\sigma/d \ll 1$ and have the same Bloch index. The nondecaying modes persist also if a real-valued periodic potential is added to the spatially periodic array of dissipations, with the period of the dissipative array being multiple of that of the periodic potential. We also consider evolution of the soliton-shaped pulses in the nonlinear Schrödinger equation with the spatially periodic dissipative lattice and find that when the pulse width is much larger than the lattice period and its wave number k is either at the center, $k = 2\pi/d$, or at the boundary, $k = \pi/d$, a significant fraction of the pulse escapes the dissipation forming a stationary nonlinear mode with the soliton shaped envelope and the Fourier spectrum consisting of two peaks centered at k and $-k$.

1. Introduction

The artificially structured materials such as photonic crystals have attracted great interest for their remarkable properties to control and manipulate light. The propagation of radiation inside a photonic crystal is affected by the periodicity in a way similar to that of an electron traveling in a periodic potential in a solid state crystal, giving rise to the photonic analog of the band structures of solid-state physics [1]. An important starting point for this analysis is the Bloch theory which provides the underlying mathematical framework for obtaining the fundamental wave propagation characteristics in photonic crystals. Through this theory, it is possible to obtain a relationship between the frequency and the wavenumber (wave vector). This relationship is referred as the frequency band structure.

On the other hand, the absorption is likely to be an essential ingredient in future photonic structures, since purely dielectric arrangements have small index variation for opening a complete bandgap below the infrared wavelengths. Indeed, there are proposals involving the metallo-dielectric structures which are promising for obtaining the complete photonic bandgap [2, 3, 4]. On the other hand, the absorptive periodic structures are not thoroughly investigated, with rather few results available. While a small absorption can only slightly modify the band structure [5], in general, the absorption turns Bloch bands into resonances in the lower-half complex plane [6, 7], resulting in attenuation of the Bloch modes. For instance, based on numerical simulations of the periodic dielectric-metallic superlattice, it was concluded that the photonic band structure is strongly modified as compared to the band structure of the nonabsorbing superlattice: the Bloch vector becomes complex for all frequencies, and the waves are evanescent [8]. However, the influence of absorption seems to be far more complex than just attenuation. Indeed, it has been known for quite some time that there are some interesting peculiarities in the effect of action of dissipation on the photonic band structures, such as the asymmetric behavior of the actual absorption rate for wave vectors near the Brillouin-zone boundary and the splitting of the lifetimes of the degenerate modes [9, 10].

Absorption attenuates the propagating modes but does this in a non-uniform way in the Fourier space of the wave numbers. Indeed, recently it was found that for a spatially periodic localized dissipation, acting on the two-dimensional real-valued periodic lattice, there are some modes featuring extremely weak dissipation, they appear for the Fourier index lying on the boundary of the Brillouin zone defined for the combined complex-valued lattice [11]. This important result was obtained for the two-dimensional lattice which did not allow full understanding of the existence of modes immune to the action of dissipation. It is of great interest to study this phenomenon in the one-dimensional case, which simplifies the analysis. Moreover, the one-dimensional case allows for a rigorous introduction of a basis of dissipative modes due to the fundamental results in the Sturm-Liouville theory [12].

Here we consider the one-dimensional linear and nonlinear Schrödinger equation

with the complex-valued potential, concentrating on the results of the action of a periodic array of spatially localized dissipations. When the local dissipation width goes to zero (while the product of the amplitude and width remain fixed), our model reduces to the complex extension of the well-known Kronig-Penney model (in the linear case), which is a text-book illustration of the Bloch bands and Bloch waves [13, 14]. The respective eigenvalue problem, i.e. the Sturm-Liouville problem with a complex-valued potential, is non-Hermitian. Fortunately, in the one-dimensional case there is a fundamental result [12] showing the existence and completeness of the (generalized, in general) eigenfunctions. This also ensures the same property for the dissipative Bloch waves, as is discussed below.

As was discussed before [11], besides application to the propagation of light in photonic crystals, our results can have applications in other branches of physics as, for instance, in the field of cold atoms and Bose-Einstein condensates in the spatially periodic traps created with laser beams, where externally controlled removal of atoms serves as dissipation (see, for instance, Refs. [15, 16], the removal of atoms can be done by a set of ordered electron beams with the use of the electron microscopy technique of Refs. [17, 18]). In the Bose-Einstein condensates, the nondecaying modes illustrate also a very slow decay of the condensate subject to an external dissipation, i.e. the quantum Zeno effect. The Zeno-like behavior in the Bose-Einstein condensates with a single dissipative defect was recently considered theoretically [19] and observed experimentally [20]. Also a macroscopic quantum Zeno effect due to nonlinear interaction in the condensate was also recently studied [21]. For instance, our results suggest that such effects can be also observed with the spatially periodic dissipation.

The rest of the text is organized as follows. In section 2 the general properties of the eigenvalue problem for a spatially periodic dissipative lattice are discussed. In section 3 the imaginary Kronig-Penney model is studied. Some mathematical details on the dissipative Bloch waves, the respective Brillouin zone, and the completeness of the Bloch wave basis are relegated to the Appendix. In section 4 we numerically study the eigenmodes of the dissipative array of localized finite-width dissipations. In sections 5 we confirm the existence of the nondecaying modes by direct numerical solution of the Schrödinger equation. In section 6 we also consider the propagation of soliton pulses in the nonlinear Schrödinger equation with the dissipative lattice. Summary of the results is given in section 7.

2. Bloch waves and Bloch bands for a dissipative lattice

We consider propagation governed by the one-dimensional Schrödinger equation and focus on the effect of a spatially periodic localized dissipation applied to a periodic potential (lattice),

$$i\partial_t\psi = -\frac{1}{2}\partial_x^2\psi + \mathcal{V}(x)\psi \equiv \mathcal{L}\psi. \quad (1)$$

It proves to be of great convenience to introduce for a periodic dissipative lattice $\mathcal{V}(x) = V(x) - iG(x)$, $\mathcal{V}(x+d) = \mathcal{V}(x)$, $V \in \mathbb{R}$ and $G \geq 0$, the Bloch waves $\psi_{n,k}(x)$ as the eigenvectors of the non-Hermitian eigenvalue problem (i.e. for a complex-valued spatially periodic potential) with the standard Bloch-like boundary condition:

$$\mathcal{L}\psi_{n,k}(x) = \mu_n(k)\psi_{n,k}(x), \quad \psi_{n,k}(x+d) = e^{idk}\psi_{n,k}(x), \quad (2)$$

where $-\pi/d < k < \pi/d$ (an analog of the Brillouin zone). Here the reciprocal lattice basis is as usual and the eigenvalue problem is considered on the unit cell of the dissipative lattice. The complex eigenvalues, $\mu_n(k) = E_n(k) - i\gamma_n(k)$ with $E_n(k) \in \mathbb{R}$ and $\gamma_n \geq 0$, enumerated by a discrete index n , represent an analog of Bloch bands (now consisting, generally, of decaying modes). Moreover, similarly to the real-valued potential case, there is a complete basis of such generalized Bloch waves (a detailed treatment of the complex-valued potential and the generalized Bloch theory can be found in the Appendix). Note also for the following that for k outside the Brillouin zone, the eigenfunction $\psi_k(x)$ is the same as that for an equivalent k inside the zone.

Our main interest lies in the spatially periodic dissipation which is sharply localized function in each period, thus a particular profile of the dissipation near its maxima is not important. We will use the Gaussian profile due to analytical simplicity, fixing its period to be 2π :

$$G(x) = G_0 \sum_{m=-\infty}^{\infty} e^{-(x-2m\pi)^2/\sigma^2}, \quad (3)$$

where the narrow-width approximation requires that $\sigma \ll 2\pi$ (previously it was established that the nondecaying modes appear in this limit [11]).

Our purpose is to find out properties of the nondecaying spatial structures governed by Eqs. (1)-(3). Due to the spatial periodicity of the dissipation, it is sometimes simpler to work in the Fourier representation. We have:

$$G(x) = \sum_{n=-\infty}^{\infty} \Gamma_n e^{-inx}, \quad \Gamma_n = \frac{\sigma G_0}{2\sqrt{\pi}} e^{-(\frac{n\sigma}{2})^2}. \quad (4)$$

By analogy with the real-valued periodic potential, one can rewrite the dissipative Bloch-like wave as $\psi_k(x) = e^{ikx}u_k(x)$, $u_k(x+2\pi) = u_k(x)$, thus the following expansion is valid

$$\psi_k(x) = e^{ikx} \sum_{n=-\infty}^{\infty} C_n(k) e^{-inx}, \quad (5)$$

where, in difference with the real-valued case, the dissipative Bloch wave corresponds to a complex eigenvalue μ . Assuming the solution $\psi_k(x, t) = e^{-i\mu t}\psi_k(x)$ with $\psi_k(x)$ of Eq. (5), we obtain the eigenvalue problem (2) in the form

$$\mu C_n = \frac{1}{2}(k-n)^2 C_n + \sum_{m=-\infty}^{\infty} (\hat{V}_{n-m} - i\Gamma_{n-m}) C_m \equiv \sum_{m=-\infty}^{\infty} L_{n,m}(k) C_m, \quad (6)$$

where \hat{V}_n is the Fourier component of the real-valued potential $V(x)$. Note that when $\sigma \ll 1$, about $1/\sigma$ terms in the Fourier series (4) have the amplitude $\Gamma_n \approx \Gamma_0$. This fact

allows for the extremely weakly decaying modes in Eq. (6), as we will see below, and the existence of such can be understood as a dissipative analog of the well-known Bragg resonance.

3. The zero-width dissipation approximation: the imaginary Kronig-Penney model

For $\sigma \rightarrow 0$ with $G_0 \sim \sigma^{-1}$ (i.e. keeping Γ_0 fixed) and $V(x) = 0$ Eq. (6) reduces to the eigenvalue problem for the Kronig-Penney model (see Ref. [13]) with an imaginary potential, since $\frac{1}{\sqrt{\pi}\sigma}e^{-\frac{x^2}{\sigma^2}} \rightarrow \delta(x)$ as $\sigma \rightarrow 0$ and we obtain

$$G(x) \rightarrow 2\pi\Gamma_0 \sum_{m=-\infty}^{\infty} \delta(x - 2m\pi). \quad (7)$$

The eigenfunctions in this limit can be easily found using the Fourier representation (6). We have for the periodic part

$$u_k(x) = -iu_k(0)\Gamma_0 \sum_{m=-\infty}^{\infty} \frac{e^{imx}}{\mu(k) - \frac{1}{2}(m+k)^2}, \quad (8)$$

where the eigenvalues are obtained from the equation

$$\sum_{m=-\infty}^{\infty} \frac{1}{\mu(k) - \frac{1}{2}(m+k)^2} = \frac{i}{\Gamma_0}. \quad (9)$$

Eq. (9) is the consistency condition for Eq. (8) and can be cast as

$$\cos(2\pi k) = \cos(2\pi\sqrt{2\mu}) - i\frac{2\pi\Gamma_0}{\sqrt{2\mu}} \sin(2\pi\sqrt{2\mu}), \quad (10)$$

by noticing that the Mittag-Leffler expansion formula (i.e. the expansion in terms of the pole singularities) for the following expression $\frac{\pi}{2\sqrt{\mu}} [\cot(\pi[\sqrt{\mu} + k]) + \cot(\pi[\sqrt{\mu} - k])]$ is the l.h.s. of Eq. (9). Eq. (10) is a complex-valued extension of that for the ordinary Kronig-Penney model (see, for instance, Ref. [14]). It shows that the Kronig-Penney model with the imaginary potential (7) allows for the nondecaying modes when $\sin(2\pi\sqrt{2\mu}) = 0$, i.e. for $k = 0$ or $k = 1/2$ with $\mu_{2n}(0) = \frac{1}{2}n^2$ and $\mu_{2n-1}(\frac{1}{2}) = \frac{1}{2}(n - \frac{1}{2})^2$, $n = 1, 2, 3, \dots$

Let us now find the structure of the corresponding nondecaying modes. Since they are eigenfunctions corresponding to the resonant points, i.e. to zeros of the denominator in Eq. (8), and satisfy also $u_k(0) = 0$ one has to deal with the undeterminate ratio of the type 0/0 (i.e. the contributing terms in the expansion of Eq. (8) are those with zero denominator). To open the indeterminacy we recall the original equation for the eigenfunctions in the Fourier space, of Eq. (6), where for $\Gamma_n = \Gamma_0$ under the condition that $\frac{1}{2}(k - n)^2 = \mu(k)$ the sum on the r.h.s. must satisfy $\sum_{n=-\infty}^{\infty} C_n(k) = u_k(0) = 0$. Hence, the nondecaying modes are given by a sum of just two resonant Fourier terms with the amplitudes $C_{n_2} = -C_{n_1}$: for $k = 0$, i.e. in the center of the Brillouin zone, we have $n_2 = -n_1$ and the nondecaying modes are $u_0(x, n) = A_n \sin(nx)$, while for $k = 1/2$,

i.e. at the boundary of the Brillouin zone, we have $n_2 = 1 - n_1$ and the nondecaying modes are $u_{\frac{1}{2}}(x, n) = B_n e^{-ix/2} \sin([n - 1/2]x)$ (here $n \equiv n_1 \in \{1, 2, 3, \dots\}$). We conclude noting that the real eigenvalues $\mu(k)$ belong either to the center or the boundary of the Brillouin zone and this resonant feature can be understood as an analog of the Bragg resonance for the spatially periodic dissipative lattice.

4. The Bloch modes in the case of a periodic array of finite-width dissipations

In the previous section we have analyzed the zero-width dissipation case and found an infinite number of nondecaying modes in the periodic array of such dissipations. Now let us consider the finite-width case. We concentrate on the following periodic lattice potential

$$\mathcal{V}(x) = V_0 \cos(2x) - iG_0 \sum_{m=-\infty}^{\infty} e^{-(x-2m\pi)^2/\sigma^2}. \quad (11)$$

Properties of the Bloch band structure of this dissipative periodic lattice crucially depend on the ratio of σ , the width of the dissipations, to the distance between the sites, i.e. the lattice period ($d = 2\pi$ in our case), and on the dissipation strength G_0 . Sometimes we will use the set of parameters σ and Γ_0 which are more appropriate in the Fourier space. All numerical simulations of this and the following sections are performed with the use of the highly accurate Fourier pseudospectral method (see, for instance, Ref. [22]). Let us present the numerical results on the band structure of the dissipative lattice in Eq. (11). Fig. 1 shows the real and imaginary parts of the Bloch bands for the lattice in Eq. (11). Note the several magnitudes difference between the imaginary components. The nondecaying modes appear only for $k = 0$ or $k = 1/2$. The dissipation also partially closes the band gaps between the bands, only the gap between the second and third bands is visible.

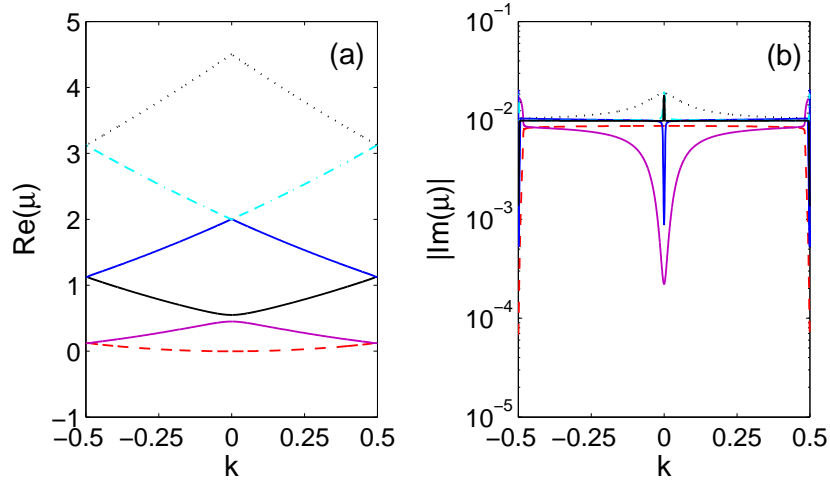


Figure 1. Panel (a), the real component of the Bloch bands. Panel (b), the imaginary component of the Bloch bands. Here $V_0 = 0.1$, $G_0 = 0.22$, $\sigma = \pi/20$, giving $\Gamma_0 = 0.01$.

Fig. 2 shows the imaginary component of Fig. 1 separately for the even and odd bands (enumerated by the real component). We can see that only three bands remain nondecaying at the center or at the boundary of the Brillouin zone (namely, the first, the second, and the fourth bands). The even bands have a nondecaying mode in the center ($k = 0$), whereas the odd band has a nondecaying mode at the boundary ($k = 1/2$), i.e. in agreement with the Kronig-Penney model, though a real-valued potential (with a compatible period) is added to the dissipation.

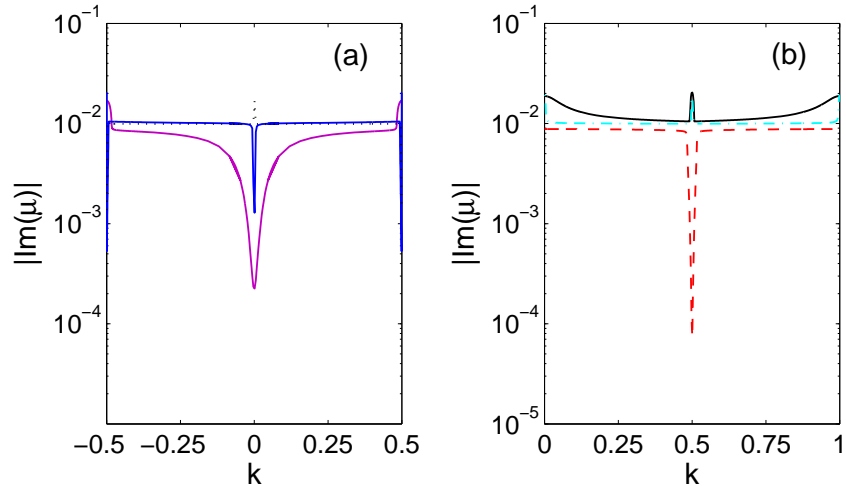


Figure 2. Panel (a), the imaginary component of the even bands. Panel (b), the same for the odd bands. The parameters are as in Fig. 1.

Thus, it becomes apparent that the main cause of the nondecaying modes in the realistic dissipative lattice ($\sigma > 0$) is the cancellation of the dissipation in the Fourier space, as it is in the imaginary Kronig-Penney model (however, the additional real lattice term can prevent some of the cancellations, as it occurred with the odd bands in Fig. 2, where there is just one odd band with nondecaying modes as compared with Fig. 4, where three odd bands have nondecaying modes). Therefore, for the rest of this section we consider the purely dissipative case, i.e. setting $V(x) = 0$. Fig. 3 confirms that for the pure periodic dissipation there are no band gaps (as in the imaginary Kronig-Penney model). Fig. 4 shows the imaginary components of the Bloch bands.

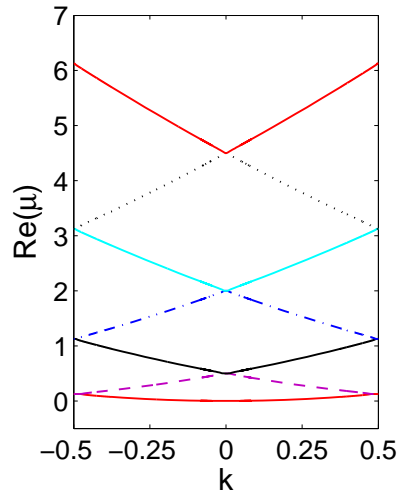


Figure 3. The real component of the Bloch bands for pure dissipative lattice. Here $V_0 = 0$, $G_0 = 1.6$, $\sigma = \pi/100$, giving $\Gamma_0 = 0.14$.

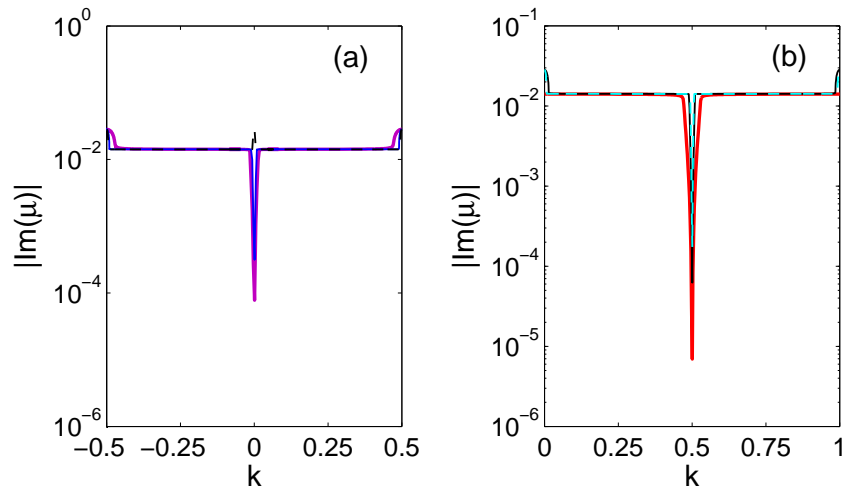


Figure 4. Panel (a), the imaginary components of the even bands. Panel (b), the same for the odd bands. The parameters are as in Fig. 3.

We note that the qualitative behavior of the Bloch bands does not change with decrease of Γ_0 , if σ is kept constant. For very small values of σ , the effects of the dissipation are the same as in the imaginary Kronig-Penney model with, however, finite dissipation of the modes in the center and at the boundary of the Brillouin zone (the dissipation is stronger in the higher bands). Increasing σ results in the increase of the

dissipation rate in all bands, the weakly decaying modes disappear from the higher bands first. All weakly decaying modes disappear as σ approaches the lattice period, compare Figs. 4 and 5. There is an additional feature for σ just an order smaller than the lattice period. For $\sigma = \pi/10$, as in Fig. 5, the higher bands have minima of the imaginary component in the switched places, i.e. the higher even bands have minima at the boundary of the Brillouin zone, see panel (a) of Fig. 5, while the higher odd bands have minima at the center, panel (b) (note that the bands are labeled by their real component as in Fig. 3).

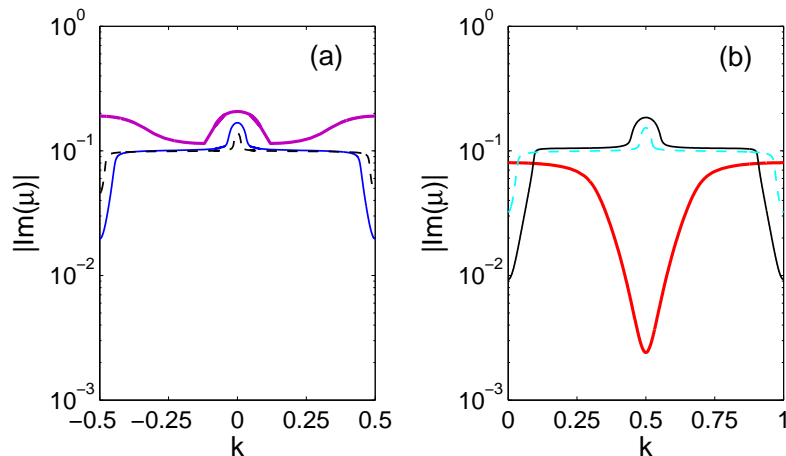


Figure 5. Panel (a) gives the real part, panel (b) gives the imaginary part. Here $V_0 = 0$, $G_0 = 1.12$, $\sigma = \pi/10$, giving a value of $\Gamma_0 = 0.1$.

Now, by keeping the value of σ constant (we chose $\sigma = \pi/10$) we observe that the effect of decreasing the parameter Γ_0 , the dissipation strength in the Fourier space, is to decrease the width of the minima of the imaginary component of the Bloch bands, besides an obvious decrease of their values, compare Figs. 5 and 6.

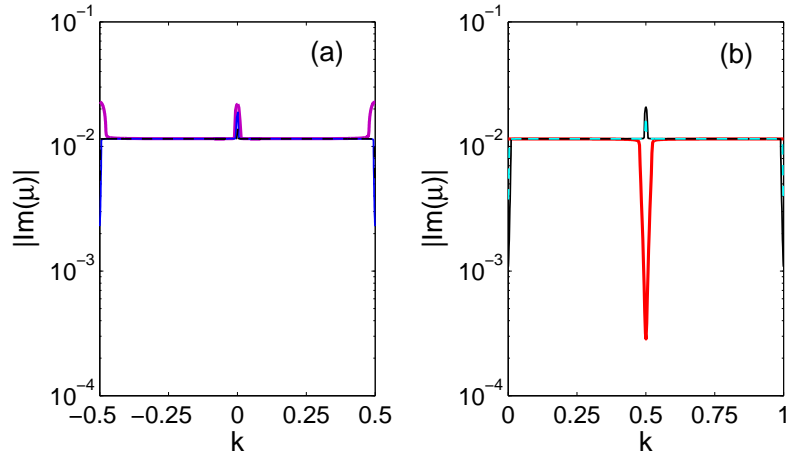


Figure 6. Panel (a), the even imaginary bands. Panel (b), the odd imaginary bands. Here $V_0 = 0$, $G_0 = 0.13$, $\sigma = \pi/10$, giving $\Gamma_0 = 0.01$

Therefore, we have established that the appearance of extremely weakly decaying Bloch modes in a periodic dissipative array of finite-width localized dissipations stems from the cancellation of the dissipations in the Fourier space of wave numbers, similarly as it is predicted by the imaginary Kronig-Penney model of section 3 (i.e. we have a dissipative analog of the Bragg resonance). For a finite dissipation width σ , only a finite number of the nondecaying modes survive (which have extremely small dissipation rates, orders of magnitude smaller than the applied dissipation rate). We have found that the width of the dissipative analog of the Bragg resonance is proportional to the strength of the dissipation in the Fourier space of wave numbers. Moreover, whereas a real-valued potential can modify the Bloch bands and prevent for some of the cancellations of the dissipation (i.e. some of the dissipative Bragg resonances) it has no influence on the Bloch indices of the weakly decaying modes. Below we consider the numerical simulations of the time-dependent Schrödinger equation with the dissipative lattice to confirm the predictions of the eigenvalue analysis.

5. Wave dynamics in the dissipative lattice

For numerical solution of the Schrödinger equation we use the so-called split-step Fourier method [22] with the pseudo-spectral approximation of the derivatives in the spatial coordinate. According to the discussion above, we focus on the purely dissipative lattice, setting $V_0 = 0$. Without any loss of generality, we can use a plane wave $\psi(x, 0) = e^{ikx}U_0$ as the initial condition. Since the dissipative lattice \mathcal{V} is periodic, evolution governed by Eq. (1) preserves the quasimomentum k and assumes the form $\psi(x, t) = e^{ikx}U(x, t)$ (see also the Appendix). We can thus simulate the time evolution on the primitive lattice

cell (simulations made on a finite lattice for the Gaussian-shaped initial condition of width much larger than the lattice period confirm this). The results are given in Fig. 7, where we plot the rescaled norm of the solution, i.e. $\|\psi\|^2 = \int |\psi(x, t)|^2 dx / \int |\psi(x, 0)|^2 dx$ (where the integration is over the lattice period 2π). One can clearly spot the presence of extremely weakly decaying modes. Moreover, they exist only for the wave index lying either in the center ($k = 1$) or at the boundary ($k = 1/2$) of the Brillouin zone (of the dissipative lattice). Here we note that Bloch modes with the wave number shifted by addition of multiples of the Fourier period $K = \frac{2\pi}{d} = 1$ belong to higher Bloch bands, thus $k \pm n$, with k in the Brillouin zone, may be nondecaying for some natural n depending on the value of σ (depending on the value of σ there are several bands with the weakly decaying modes, as is discussed in the previous section).

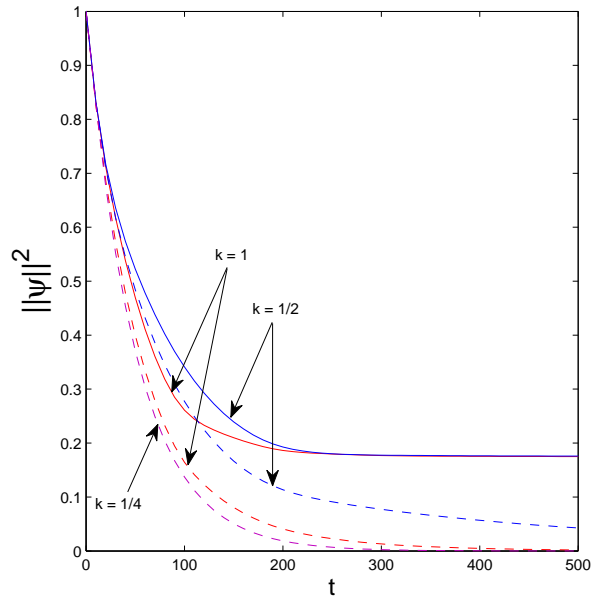


Figure 7. The norm of the solution for the initial condition $\Psi(x, 0) = e^{ikx}U_0$. We use several Bloch indices: $k = 1$, $k = 1/2$, and $k = 1/4$, for two values of (σ, G_0) (and one for $k = 1/4$): $\sigma = \pi/100$ and $G_0 = 1.13$ (solid lines) and $\sigma = \pi/4$ and $G_0 = 0.045$ (dashed lines). Here $V_0 = 0$ and $\Gamma_0 = 0.01$.

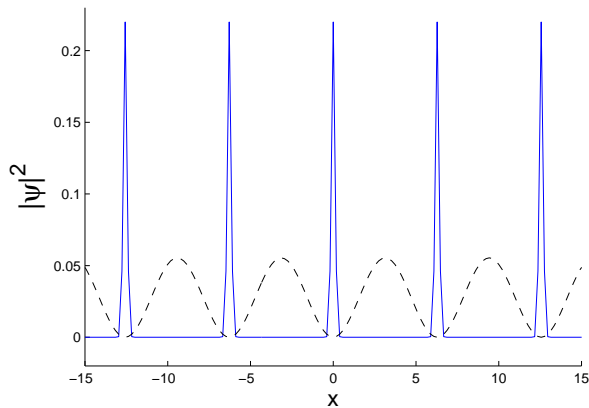


Figure 8. The spatial profile of the nondecaying wave solution. We show the dissipative sites (the solid line) and the solution (the dashed line). The parameters correspond to one curve from Fig. 7, namely, $k = 1/2$, $\sigma = \pi/100$, $G_0 = 1.13$, and $\Gamma_0 = 0.01$.

As the nondecaying Bloch mode must approach zero at the maxima of the dissipation, i.e. in intervals of size on the order of σ , the nondecaying waves of Fig. 7 have periodic variation of the absolute value with period of the dissipative array, see Fig. 8. They are linear combination of the weakly decaying Bloch modes present in the lower bands.

6. Nonlinear wave dynamics in dissipative lattice

Consider now propagation of nonlinear waves governed by the nonlinear Schrödinger equation with the periodic dissipative lattice, i.e.

$$i\partial_t\Psi = -\frac{1}{2}\partial_x^2\Psi + \mathcal{V}(x)\Psi - g|\Psi|^2\Psi. \quad (12)$$

Setting $V = 0$ (i.e. considering the purely dissipative lattice) and $g > 0$ (to allow for the soliton solutions for zero dissipation), let us focus on the effect of a spatially periodic dissipation on the nonlinear wave dynamics.

Our model can be considered as a finite-width extension of an imaginary variant of the nonlinear Kroning-Penney model. The existence of localized (soliton-like) and extended (Bloch-like) nonlinear modes in the usual nonlinear Kroning-Penney model (i.e. with a real-valued potential) was studied before (see for instance, Refs. [23, 24] and references therein), where exact solutions were found. Here we also note that in the case when $V(x)$ is a real-valued periodic potential (not necessarily localized within each period) Eq. (12) possesses the so-called gap soliton solutions, due to the fact that they appear in the band gaps of the Bloch spectrum of the periodic potential. The gap solitons were first discovered in optics [25, 26] (see also a book [27]) and then predicted [28] and observed experimentally in the quasi one-dimensional Bose-Einstein condensates [29]. In contrast, the periodic dissipation does not lead to the band gaps,

thus our nonlinear waves, which are discussed below, are quite different from both the gap solitons and the nonlinear Bloch modes studied before.

We find that there are nonlinear extremely weakly decaying modes, i.e. nonlinear waves immune to the applied periodic dissipation, see Fig. 9. As the initial condition we have used the usual soliton profile $\Psi(x, 0) = e^{ikx} A \sqrt{\frac{2}{g}} \text{sech}(Ax)$, of the nonlinear Schrödinger equation (note that $A = 1/l$, where l is the width of the soliton). When $l \sim 2\pi$ all waves decay, see Fig. 9(a), whereas for $l \gg 2\pi$ the waves with the wave index in the center of the Brillouin zone of the dissipative lattice (we use $k = 1$) and at its boundary ($k = 1/2$) are almost immune to the dissipation, see Fig. 9(b).

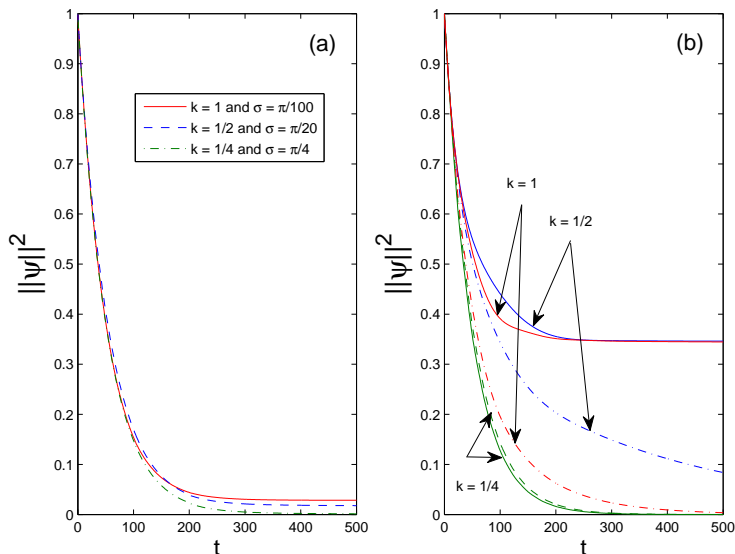


Figure 9. Panel (a), the norm of the solution for $g = 1$ and the initial condition $\Psi(x, 0) = e^{ikx} A \sqrt{\frac{2}{g}} \text{sech}(Ax)$ with $A = 1/\pi$. Panel (b), the norm of the solution when $A = 1/(10\pi)$. We use several Bloch indices: $k = 1$, $k = 1/2$, and $k = 1/4$, for three values of (σ, G_0) : $\sigma = \pi/100$ and $G_0 = 1.13$ (the solid lines), $\sigma = \pi/20$ and $G_0 = 0.22$ (the dashed lines), and $\sigma = \pi/4$ and $G_0 = 0.045$ (the dash-dotted lines). In all cases $\Gamma_0 = 0.01$.

The nondecaying nonlinear waves in the dissipative lattice can be considered as analogs of the soliton solutions of the usual (i.e. conservative) nonlinear Schrödinger equation. Indeed, in Fig. 10 we show the spatial structure of such a nonlinear nondecaying wave in the dissipative lattice. Fig. 10(b) shows that the spatial envelope of the nondecaying nonlinear wave has the soliton shape. In Fig. 10 we use $k = 1/2$, but for $k = 1$ the result is very similar (in both cases there are extremely weakly decaying nonlinear waves in the model, as shown in Fig. 9(b)). Moreover, to verify that the nonlinear wave of Fig. 10 contains the nonlinear eigenvalue of the Riemann-Hilbert problem associated with the canonical nonlinear Schrödinger equation, and thus indeed contains a soliton, we have numerically verified the respective sufficient condition [30],

which is formulated as follows

$$I(t) = \int_{-\infty}^{\infty} dx |\psi(x, t)| \geq \ln(2 + \sqrt{3}). \quad (13)$$

Condition (13) must be satisfied for large values of t , if the soliton part is present in the nonlinear wave. Here we note that condition (13) is formulated only for the nonlinear Schrödinger equation without the dissipative lattice, however, one can use the nonlinear spectrum provided by the Riemann-Hilbert problem to judge about the presence of a soliton component in the solution for the perturbed equation, similarly as it was done in Ref. [31] for an exact treatment of the soliton-radiation interaction in a nonintegrable evolution equation of the nonlinear Schrödinger type. We have verified that in the case of the nonlinear wave of Fig. 10, and in all other cases, when the localized wave survives the dissipation, the behavior of $I(t)$ is as follows: it initially rapidly decreases (for instance, in the case of Fig. 10 on an interval $t \sim 10$) to a constant value well satisfying condition (13) and then stays almost constant.

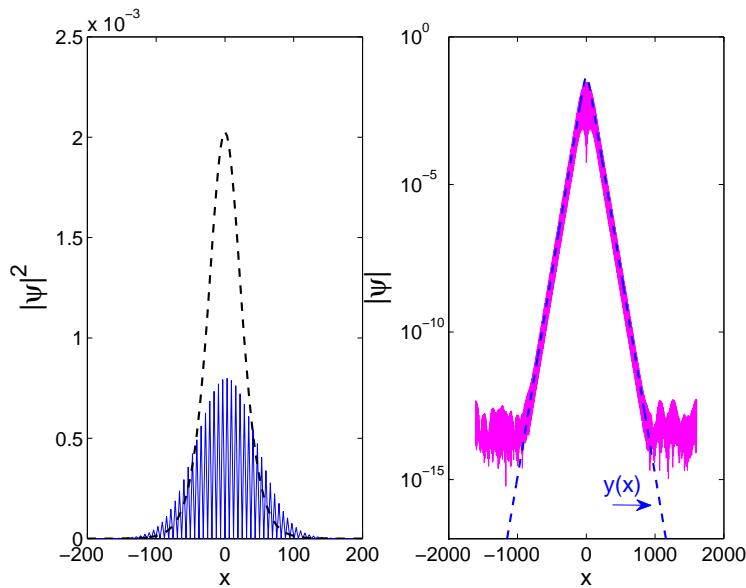


Figure 10. Panel (a), the nonlinear (soliton) wave solution for the initial time (the dashed line) and at a much larger time (the solid line). Panel (b), the envelope of the solution at a large time (the solid line) compared with $y(x) = A_1 \sqrt{\frac{2}{g}} \text{sech}(A_1 x)$ with $A_1 = \max(|\psi(x, 500)|)$ (the dashed line). Here $k = 1/2$, $A = 1/(10\pi)$, $\sigma = \pi/100$, and $G_0 = 1.13$.

Finally, we note that the soliton waves with the wave number k lying at the center or on the boundary of the Brillouin zone (for instance, we used $k = 1/2$ and $k = 1$) is attracted to a *stationary* (extremely weakly decaying) nonlinear mode. This

is illustrated in Fig. 11, where we plot the time evolution of the pulse mean position

$$\langle x \rangle = \frac{\int dx x |\Psi|^2}{\int dx |\Psi|^2}. \quad (14)$$

One can clearly see the signatures that the solution first acquires some negative Fourier components (which results in the spatial oscillations of the mean position) and then settles at a stationary position in the dissipative lattice. Moreover, we have verified that the Fourier spectrum of the stationary nonlinear mode is indeed composed of k and $-k$ peaks of equal amplitude, as one would expect from the above analysis due to periodicity of the array of dissipations. Thus, the stationary mode can be rightfully called a bound soliton, due to its soliton-shaped envelope and the symmetric Fourier spectrum about the origin.

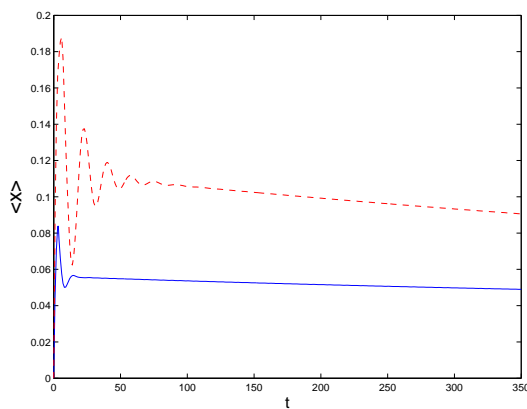


Figure 11. The spatial position of the nonlinear wave. Here $k = 1/2$ (the solid line) and $k = 1$ (the dashed line). The other parameters are as in Fig. 9.

7. Conclusion

We have found the existence of extremely weakly decaying linear and nonlinear waves in the one-dimensional spatially periodic array of localized dissipations, when the dissipation width is much smaller than the array period. The origin of such nondecaying modes was established by considering the zero-width limit of the model, which is a complex-valued generalization of the well-known Kronig-Penney model of the solid state physics. The Kronig-Penney model with an imaginary potential allows for an infinite number of nondecaying Bloch modes with the wave index lying either at the center or at the boundary of the corresponding Brillouin zone (a generalization of the usual concept for the complex-valued potential). We have numerically confirmed that the nondecaying (i.e. almost nondecaying in this case) modes persist in the periodic array of finite-width dissipations, however, only a few lowest Bloch bands allow for such modes for the dissipations of a finite width. The lower-band nondecaying modes survive if a real-valued potential is added to the dissipative lattice, when the period of the dissipative array is multiple of that of the real-valued potential. Numerical simulations

of the governing Schrödinger equation confirm the existence of the linear waves immune to the dissipation. Moreover, we have studied the nonlinear Schrödinger equation, which allows for the soliton solutions in the absence of the dissipation, and found that a significant portion of the soliton pulse survives the dissipative lattice forming a novel stationary nondecaying nonlinear wave. Moreover, the envelope of the emerging nonlinear stationary wave is of the soliton shape, it has the symmetric Fourier spectrum with respect to the index inversion and thus can be rightfully called the soliton bound state of the model, which is immune to the dissipation. The results can have immediate applications in the propagation of optical pulses in the photonic crystals and in the field of cold atoms and Bose-Einstein condensates in the periodic optical lattices.

8. Acknowledgements

VSS was supported by the CNPq and SCF was supported by the CAPES of Brazil.

Appendix A. The Bloch wave theory generalized to the spatially periodic dissipative lattice

Similar as is in the case of the usual Bloch waves in a real-valued potential, the dissipative Bloch waves can be used for expansion of an arbitrary function $f(x)$, decaying for large x at least as $\sim |x|^{-3}$, if we allow for the generalized Bloch-wave solutions to the eigenvalue problem, $\psi_{k,n}^{(s)}(x)$, labeled by an index s for each eigenvalue. They satisfy

$$\mathcal{L}\psi_{k,n}^{(s)}(x) = \mu_n(k)\psi_{k,n}^{(s)}(x) + \psi_{k,n}^{(s-1)}(x), \quad \psi_{n,k}^{(s)}(x+d) = e^{idk}\psi_{n,k}^{(s)}(x), \quad (\text{A.1})$$

where $\mathcal{L} = -\frac{1}{2}\partial_x^2 + \mathcal{V}(x)$ with a complex-valued periodic potential $\mathcal{V}(x)$, $\psi_{k,n}^{(0)}(x) \equiv \psi_{k,n}(x)$ is the analog of the usual Bloch wave (i.e. the eigenmode to which a Bloch wave transforms when a periodic dissipation of infinitesimal amplitude is added to the real-valued lattice potential). Indeed, assuming the period of the combined complex-valued lattice to be $d = 2\pi$, the Fourier representation of $f(x)$ can be transformed as follows

$$f(x) = \int_{-\infty}^{\infty} dk e^{ikx} \hat{f}(k) = \int_{-\frac{1}{2}}^{\frac{1}{2}} dk e^{ikx} \hat{F}(k, x), \quad (\text{A.2})$$

where we have identified $\hat{F}(k, x) = \sum_{n=-\infty}^{\infty} e^{inx} \hat{f}(k + nk)$, which is periodic function in x : $\hat{F}(k, x + 2\pi) = \hat{F}(k, x)$. By a well-known result on the generalized Sturm-Liouville problem for a complex-valued periodic potential [12], the spatially periodic function $\hat{F}(k, x)$ can be expanded over the basis of the generalized eigenvectors of the non-Hermitian Sturm-Liouville problem, formulated for \mathcal{L} on the interval $x \in [0, 2\pi]$ (moreover, the multiplicity m_n of each complex eigenvalue $\mu_n(k)$ is finite, i.e. $0 \leq s \leq m_n$ in Eq. (A.1)). That is to say that $e^{ikx} \hat{F}(k, x)$ can be expanded over the basis of the

generalized Bloch waves $\psi_{k,n}^{(s)}(x)$ with a fixed k , where the index n enumerates the eigenvalues $\mu_n(k)$. Therefore, we get the expansion for an arbitrary $f(x)$:

$$f(x) = \int_{-\frac{1}{2}}^{\frac{1}{2}} dk \sum_{n=1}^{\infty} \sum_{s=0}^{m_n} b_{n,s}(k) \psi_{k,n}^{(s)}(x). \quad (\text{A.3})$$

The coefficients $b_{n,s}(k)$ can be obtained by using the inner product with the eigenvectors of the adjoint (i.e. Hermitian conjugated) eigenvalue problem, formulated for $\mathcal{L}^\dagger = \mathcal{L}^*$:

$$\mathcal{L}^\dagger \tilde{\psi}_{k,n}^{(s)}(x) = \mu_n^*(-k) \tilde{\psi}_{k,n}^{(s)}(x) + \tilde{\psi}_{k,n}^{(s-1)}(x) \quad (\text{A.4})$$

with the same Bloch-type boundary condition. The adjoint eigenvectors are related to the eigenvectors of \mathcal{L} by

$$\tilde{\psi}_{k,n}^{(s)}(x) = (\psi_{-k,n}^{(s)}(x))^*. \quad (\text{A.5})$$

Eq. (A.4) simplifies for a potential satisfying the inversion property $\mathcal{V}(-x) = \mathcal{V}(x+a)$ (satisfied by our dissipative lattice). Indeed, we have in this case $\mu_n(-k) = \mu_n(k)$. The inner product relations can be established by a standard procedure with the use of Eqs. (A.1) and (A.4), they read

$$\begin{aligned} \int_{-\infty}^{\infty} dx (\tilde{\psi}_{k',n'}^{(\tau)}(x))^* \psi_{k,n}^{(s)}(x) &= \int_{-\infty}^{\infty} dx \tilde{\psi}_{-k',n'}^{(\tau)}(x) \psi_{k,n}^{(s)}(x) \\ &= \delta(k-k') \delta_{n',n} \delta_{\tau,m_n-s}. \end{aligned} \quad (\text{A.6})$$

For example, a solution to the linear Schrödinger equation $i\partial_t U(x,t) = \mathcal{L}U(x,t)$ can be expanded over the dissipative Bloch waves as follows

$$U(x,t) = \int_{-\frac{1}{2}}^{\frac{1}{2}} dk \sum_{n=1}^{\infty} e^{-i\mu_n(k)t} \sum_{s=0}^{m_n} \frac{(-it)^s}{s!} b_{n,s}(k) \psi_{k,n}^{(s)}(x), \quad (\text{A.7})$$

where

$$b_{n,s}(k) = \int_{-\infty}^{\infty} dx \psi_{-k,n}^{(m_n-s)}(x) U(x,0). \quad (\text{A.8})$$

Note that only weakly or nondecaying Bloch waves are important for the long-time behavior of solutions to the Schrödinger equation. Thus one does not need to characterize all the generalized eigenvectors, restricting oneself only to the weakly decaying ones.

In difference with the Hermitian eigenvalue problem, generally, the generalized eigenvectors are common, they are solutions to Eq. (A.1) (i.e. the multiplicity $m_n > 0$ for some $\mu_n(k)$). However, their appearance is conditioned on that

$$\int_0^{2\pi} dx u_{-k,n}(x) u_{k,n}(x) = 0, \quad (\text{A.9})$$

which follows from Eq. (A.6).

Now let us return to the specific eigenvalue problem (6) of section 2. First of all, we note that the operator \mathcal{L} (1) is symmetric with respect to inversion $x \rightarrow -x$, resulting in $L_{n,m}(k) = L_{m,n}(k)$, thus $u_{-k,n}(x) = u_{k,n}(-x)$, $C_n(-k) = C_{-n}(k)$. Hence, the orthogonality for the proper eigenvectors in Eq. (A.6) simplifies to

$$\sum_{n=-\infty}^{\infty} C'_n(k)C_n(k) = 0, \quad \mu'(k) \neq \mu(k), \quad (\text{A.10})$$

and a similar sum appears in condition (A.9) for the generalized eigenvectors. Condition (A.9) was checked numerically in our case, we have found no generalized eigenvectors for the eigenvalues $\mu(k)$ which correspond to the weakly decaying modes, i.e. the mode of our principal interest.

References

- [1] Madelung O 1978 *Introduction to Solid-State Theory* (Springer-Verlag, Berlin Heidelberg)
- [2] Moroz A 1993 Phys. Rev. Lett. **83** 5274
- [3] Moroz A 2000 Europhys. Lett. **50** 466
- [4] van der Lem H and Moroz A 2000 J. Opt. A: Pure Appl. Opt. **2** 395
- [5] Krokhin A and Halevi P 1996 Phys. Rev. B **53** 3
- [6] Tip A, Moroz A and Combes J-M 2000 J. Phys. A: Math. Gen. **33** 6223
- [7] Moroz A, Tip A and Combes J-M 2001 Synthetic Metals **116** 481
- [8] Soto-Puebla D, Xiao M and Ramos-Mendieta F 2004 Physics Letters A **326** 273
- [9] Kuzmiak V and Maradurin A 1997 Phys. Rev. B. **55** 7427
- [10] Kuzmiak V and Maradurin A 1998 Phys. Rev. B. **58** 7230
- [11] Shchesnovich V S and Konotop V V 2012 Euro Phys. Lett. **99** 60005
- [12] Marchenko V A 1986 *Sturm-Liouville Operators and Applications (Operator Theory Advances and Applications)* (Birkhuser Verlag)
- [13] Kronig R L and Penney W G 1931 Proc. R. Soc. London A **130** 499
- [14] Singh S 1983 Am. J. Phys. **51** 179; Domínguez-Adame F 1987 Am. J. Phys. **55** 1003; Pedersen F B, Einevoll G T and Hemmer P C 1991 Phys. Rev. B **44** 5470
- [15] Brazhnyi V A, Konotop V V, Pérez-García V M and Ott H 2009 Phys. Rev. Lett. **102** 144101
- [16] Shchesnovich V S 2012 Phys. Rev. A **85** 053616
- [17] Gericke T, Urfeld C, Hommerstad N, and Ott H 2006, Las. Phys. Lett. **3** 415
- [18] Gericke T, Würtz P, Reitz D, Langen T, and Ott H 2008, Nat. Phys. **4** 949
- [19] Zezyulin D A, Konotop V V, Barontini G, and Ott H 2012 Phys. Rev. Lett. **109** 020405
- [20] Barontini G, Labouvie R, Stubenrauch F, Vogler A, Guarrera V, and Ott H 2013 Phys. Rev. Lett. **110** 035302
- [21] Shchesnovich V S and Konotop V V 2010 Phys. Rev. A **81** 053611
- [22] Fornberg B 1996 *A Practical Guide to Pseudospectral Methods* (Cambridge University Press, Cambridge, UK); Trefethen L N 2000 *Spectral Methods in Matlab* (SIAM, Philadelphia, PA)
- [23] Seaman B T, Carr L D, and Holland M J, 2005 Phys. Rev. A **71** 033622
- [24] Sukhorukov A A and Kivshar Yu S 2001 Phys. Rev. Lett. **87** 083901
- [25] de Sterke C M and Sipe J E 1994 Prog. Opt. **33** 203
- [26] Eggleton B J *et al* 1996 Phys. Rev. Lett. **76** 1627
- [27] Kivshar Yu S and Agrawal G P, 2003 *Optical Solitons: From Fibers to Photonic Crystals* (Academic Press, Elsevier Science).
- [28] Meystre P, 2001 *Atom Optics* (Springer-Verlag, New York) p. 205 and references therein
- [29] Eiermann B *et al*, 2004 Phys. Rev. Lett. **92** 230401

- [30] Novikov S P, Manakov S V, Pitaevski L P, and Zakharov V E 1984 *Theory of Solitons: The Inverse Scattering Method* (Consultants Bureau, New York)
- [31] Shchesnovich V S and Barashenkov I V, 2002 *Physica D* **164** 83